ChemComm

RSC Publishing

COMMUNICATION

Asymmetric cleavage of 2,2′-pyridil to a picolinic acid anion radical coordinated to ruthenium(II): splitting of water to hydrogen†

Cite this: *Chem. Commun.*, 2013, **49**, 4522

Received 4th February 2013, Accepted 25th March 2013

DOI: 10.1039/c3cc40956b

www.rsc.org/chemcomm

Manas Kumar Biswas,[a] Sarat Chandra Patra,[a] Amarendra Nath Maity,[b] Shyue-Chu Ke,[b] Thomas Weyhermüller[c] and Prasanta Ghosh*[a]

The Ru(II)–H and water promoted asymmetric cleavage of 2,2′-pyridil to pyridine-2-carbaldehyde and unprecedented picolinic acid anion radical ($PyCOOH^{-\bullet}$) complexes, which in solution produce H_2 gas and diamagnetic picolinate complexes of ruthenium(II) in moderate yields, is reported.

Like aromatic *o*-benzoquinone, 1,2-diketone is redox non-innocent and its participation in electron transfer reaction is a subject of investigation in chemical science.[1] Because of the coordinating pyridine nitrogen and keto oxygen atoms, 2,2′-pyridil [$(PyCO)_2$] with a low-lying π* orbital (LUMO) can serve as a bidentate or a multidentate π-acceptor chelating agent. Transfer of electrons to $(PyCO)_2$ is possible *via* either OO- (as a 1,2-diketone acceptor) or NO-chelating (as a keto–imine acceptor) routes as shown in Scheme S1 (ESI†). Expecting for a new multi-electron transfer product of $(PyCO)_2$ incorporating two types of electron transfer sites, soft transition metal reducing equivalent, ruthenium(II) hydride with π-acidic CO and bulkier PPh_3 as coligands has been used in a boiling aromatic hydrocarbon solvent. The result that leads to the asymmetric cleavage of the –C(O)–C(O)– bond of the coordinated $(PyCO)_2$ in the presence of moisture, oxidizing one C═O group to –COOH and transforming another C═O group to –CHO by proton reduction, is unprecedented.

In this article, we report that the reaction of $[Ru^{II}(PPh_3)_3(CO)(H)Cl]$ (**1**) with $(PyCO)_2$ in boiling moist toluene leads to the asymmetric cleavage of the –C(O)–C(O)– bond producing pyridine-2-carbaldeyde (PyCHO) as one of the products. The redox reaction progresses producing hitherto unknown dark blue picolinic acid anion radical ($PyCOOH^{-\bullet}$) complexes of type *trans*-$[Ru^{II}(PPh_3)_2(PyCOOH^{-\bullet})(CO)Cl]$ (*t*-**2**^{rad}) as a major and *cis*-$[Ru^{II}(PPh_3)_2(PyCOOH^{-\bullet})(CO)Cl]$ (*c*-**2**^{rad}) as a minor product. The reactions occurs *via* the homolytic cleavage[2] of the Ru^{II}–H bond forming a 2,2′-pyridil anion radical $[(PyCO)_2^{-\bullet}]$ complex of ruthenium(II), $[Ru^{II}(PPh_3)_2(PyCO)_2^{-\bullet}(CO)Cl]$ (**A**^{rad}), as an intermediate that is detected in a reaction with dry toluene (eqn (1)). Upon addition of H_2O, **A**^{rad} converts to *t*-**2**^{rad} and *c*-**2**^{rad} (eqn (2)). The acid anion radical complexes, *t*-**2**^{rad} and *c*-**2**^{rad}, are unstable in solutions and undergo electron transfer reactions evolving H_2 gas, eventually furnishing yellow diamagnetic picolinate ($PyCOO^-$) complexes of types *trans*-$[Ru^{II}(PPh_3)_2(PyCOO^-)(CO)Cl]$ (*t*-**3**^{ac}) and *cis*-$[Ru^{II}(PPh_3)_2(PyCOO^-)(CO)Cl]$ (*c*-**3**^{ac}) in moderate yields (eqn (3) and (4)) as depicted in Scheme 1. This unexpected reaction that has eventually led to the reduction of H_2O to H_2 by metal complexes is worth investigating in chemical science for sustainable and renewable sources of energy.[3] In this water reduction process $(PyCO)_2$ acts as an electron transfer agent undergoing asymmetric cleavage and affording acid anion radical complexes (eqn (1)–(4)). The related products were analyzed by UV-vis/NIR absorption spectra, EPR spectra of **A**^{rad}, *t*-**2**^{rad} and *c*-**2**^{rad} and single crystal X-ray structure determination of *c*-**3**^{ac}·$\frac{1}{2}$toluene including the DFT and TD DFT calculations on $[Ru(PMe_3)_2((PyCO)_2^{-\bullet})(CO)Cl]$ (**A**$^{rad}_{Me}$), *trans*-$[Ru(PMe_3)_2(PyCOOH^{-\bullet})(CO)(Cl)]$

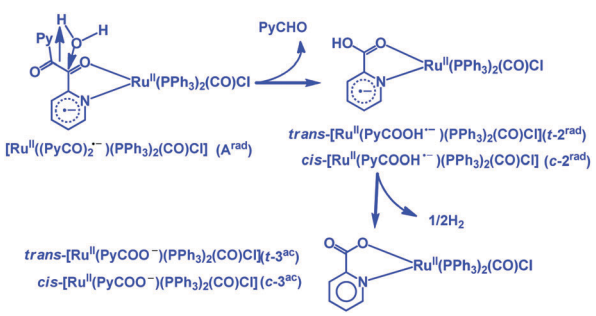

Scheme 1

[a] *Department of Chemistry, R. K. Mission Residential College, Narendrapur, Kolkata-103, India. E-mail: ghosh@pghosh.in; Fax: +91 33 2477 3597; Tel: +91 33 2428 7347*

[b] *Department of Physics, National Dong Hwa University, Shou-Feng, Hualien 97401, Taiwan*

[c] *Max-Planck Institute for Chemical Energy Conversion, Stiftstr. 34-36, 45470 Mülheim an der Ruhr, Germany*

† Electronic supplementary information (ESI) available: Syntheses, binding modes of 2,2-pyridil (Scheme S1), HPTLC analyses (Fig. S1), H_2 detection (Fig. S2), IR spectra (Fig. S3–S5), UV-vis/NIR absorption spectra (Fig. S6), redox potentials (Table S1), cyclic voltammograms (Fig. S7 and S8), kinetic isotope effects (Fig. S9 and S10), EPR spectrum (Fig. S11), optimized geometries (Fig. S12), UV-vis spectral change (Fig. S13), photoactive orbitals (Fig. S14), crystallographic data (Table S2), disordered ORTEP plot (Fig. S15), experimental bond parameters (Table S3), optimized bond parameters (Table S4), comparative bond lengths (Chart S1), electronic transition (TD DFT calculations) analyses (Table S5) and optimized coordinates (Tables S6–S10). CCDC 833917. For ESI and crystallographic data in CIF or other electronic format see DOI: 10.1039/c3cc40956b

(t-$\mathbf{2}^{rad}_{Me}$), c-$\mathbf{2}^{rad}$ and *cis*-[Ru(PMe$_3$)$_2$(PyCOOH$^{-\bullet}$)(CO)(Cl)] (c-$\mathbf{2}^{rad}_{Me}$) with a doublet spin state and *cis*-[Ru(PMe$_3$)$_2$(PyCOO$^-$)(CO)Cl] (c-$\mathbf{3}^{ac}_{Me}$) with a singlet spin state.

$$1 + (PyCO)_2 \rightarrow A^{rad} + PPh_3 + 1/2H_2 \quad (1)$$

$$A^{rad} + H_2O \rightarrow t\text{-}2^{rad} + c\text{-}2^{rad} + PyCHO \quad (2)$$

$$t\text{-}2^{rad} \rightarrow t\text{-}3^{ac} + 1/2H_2 \quad (3)$$

$$c\text{-}2^{rad} \rightarrow c\text{-}3^{ac} + 1/2H_2 \quad (4)$$

The cleavage reactions and H_2 evolution established in this investigation are shown in Scheme 1. Reaction of **1** with $(PyCO)_2$ in boiling moist toluene results in unexpected dark blue solution.† In stepwise searching, reaction of $(PyCO)_2$ with **1** in boiling dry toluene under argon affords dark brown solution due to formation of [Ru^{II}(PPh$_3$)$_2$((PyCO)$_2^{\bullet-}$)(CO)Cl] ($\mathbf{A}^{rad}$), an analogue of a 9,10-phenanthrenesemiquinone radical complex[2] as an intermediate. The geometry (*trans* or *cis*) of $\mathbf{A}^{rad}$ has not been successfully assigned. However, the formation of it in solution was detected by mass and EPR (*vide infra*) spectra. Upon addition of one drop of water, the brown solution turned dark blue and the reaction mixture was refluxed for further 10 min and cooled at 298 K. A dark blue solid of the picolinic acid anion radical complex, *trans*-[Ru^{II}(PPh$_3$)$_2$(PyCOOH$^{\bullet-}$)(CO)Cl] (t-$\mathbf{2}^{rad}$), separated out, which was filtered. The filtrate was evaporated under vacuum, and a bluish-green mass of *cis*-[Ru^{II}(PPh$_3$)$_2$(PyCOOH$^{\bullet-}$)(CO)Cl] (c-$\mathbf{2}^{rad}$) was collected. Mass, UV-vis/NIR and EPR spectra of t-$\mathbf{2}^{rad}$ and c-$\mathbf{2}^{rad}$ were recorded (*vide infra*). In solution, t-$\mathbf{2}^{rad}$ and c-$\mathbf{2}^{rad}$ radical complexes liberate H_2 molecules and were themselves transformed to yellow diamagnetic picolinate (PyCOO$^-$) complexes of types *trans*-[Ru^{II}(PPh$_3$)$_2$(PyCOO$^-$)(CO)Cl] (t-$\mathbf{3}^{ac}$) and *cis*-[Ru^{II}(PPh$_3$)$_2$(PyCOO$^-$)(CO)Cl] (c-$\mathbf{3}^{ac}$) in moderate yields as given in Scheme 1. Since, t-$\mathbf{2}^{rad}$ and c-$\mathbf{2}^{rad}$ liberate H_2 because of intra-electron transfer, crystallization of these reactive radical complexes even in argon did not succeed. The transformation of c-$\mathbf{2}^{rad}$ to c-$\mathbf{3}^{ac}$ is faster than that of the *trans*-analogue. Formation of the picolinate complexes was confirmed by single crystal X-ray structure determination of c-$\mathbf{3}^{ac}\cdot\frac{1}{2}$toluene. However, a suitable CIF for t-$\mathbf{3}^{ac}$ could not be made. t-$\mathbf{3}^{ac}$ was isolated by diffusion of *n*-hexane to the dichloromethane solution of t-$\mathbf{2}^{rad}$. c-$\mathbf{3}^{ac}\cdot\frac{1}{2}$toluene has been isolated as single crystals from the toluene solution of c-$\mathbf{2}^{rad}$. The formation of pyridine-2-carbaldeyde (PyCHO) as another important cleaved product was confirmed by HPTLC experiments with the filtrate of the reaction (ESI,† Fig. S1) and the EI mass spectrum. The evolution of H_2 gas was confirmed using GC. The gas evolved was injected into the GC instrument. H_2 was identified by an exact match with the retention time of an authentic sample (Fig. S2, ESI†).

The IR spectra (Fig. S3–S5, ESI†) and mass spectra confirm the presence of $(PyCO)_2$ in $\mathbf{A}^{rad}$. No cleavage occurs at this stage. However, the IR spectra of t-$\mathbf{2}^{rad}$ and c-$\mathbf{2}^{rad}$ are superimposable to those of the diamagnetic picolinate complexes, t-$\mathbf{3}^{ac}$ and c-$\mathbf{3}^{ac}\cdot\frac{1}{2}$toluene and the IR spectra do not support the presence of the PyCO function in t-$\mathbf{2}^{rad}$ and c-$\mathbf{2}^{rad}$ complexes. It is to be noted that because of the mixing with the acid analogue, the IR spectrum of c-$\mathbf{2}^{rad}$ displays two overlapping metal carbonyl frequencies at 1922 and 1943 cm^{-1} while only one $\nu_{C\equiv O}$ at 1943 cm^{-1} is observed for t-$\mathbf{2}^{rad}$. The molecular composition of t-$\mathbf{2}^{rad}$ and c-$\mathbf{2}^{rad}$ (m/z of [M + Na]$^+$ at 835.53, 833.53 and [M − Cl] at 777.60) differs from that of t-$\mathbf{3}^{ac}$ and c-$\mathbf{3}^{ac}$ (m/z of [M + Na]$^+$ at 834.07 and [M − Cl] at 776.10) only by a proton and is hard to affirm its existence by mass spectra. However, the mass spectra correlate the cleavage of the 2,2′-pyridil with a picolinic acid fragment.

Table 1 UV-Vis/NIR spectral data of the complexes in CH_2Cl_2 at 298 K

Compound	λ_{max}/nm (ε/10^4 M^{-1} cm^{-1})
t-$\mathbf{2}^{rad}$	762 (0.28), 687 (0.35), 631 (0.28), 577 (0.18), 528 (0.13)
c-$\mathbf{2}^{rad}$	770 (0.28), 697 (0.24), 632 (0.22), 578 (0.20), 536 (0.18)
t-$\mathbf{3}^{ac}$	762 (0.008), 684 (0.011), 634 (0.010)
c-$\mathbf{3}^{ac}$	767 (0.006), 691 (0.007), 629 (0.006)

The UV-vis/NIR absorption spectra of t-$\mathbf{2}^{rad}$, c-$\mathbf{2}^{rad}$, t-$\mathbf{3}^{ac}$ and c-$\mathbf{3}^{ac}$ in CH_2Cl_2 are recorded at 298 K. The spectra are shown in Fig. S6 (ESI†) and the data are summarized in Table 1. The lower energy absorption bands of the picolinic acid anion radical complexes, t-$\mathbf{2}^{rad}$ and c-$\mathbf{2}^{rad}$, completely disappear in the case of acid complexes, t-$\mathbf{3}^{ac}$ and c-$\mathbf{3}^{ac}$. The radical centred excitations as the origin of these lower energy absorptions of t-$\mathbf{2}^{rad}$ and c-$\mathbf{2}^{rad}$ complexes have been elucidated by TD DFT calculations on *trans*-[Ru(PMe$_3$)$_2$(PyCOOH$^{-\bullet}$)(CO)(Cl)] (t-$\mathbf{2}^{rad}_{Me}$) and *cis*-[Ru(PMe$_3$)$_2$(PyCOOH$^{-\bullet}$)(CO)(Cl)] (c-$\mathbf{2}^{rad}_{Me}$) (*vide infra*) complexes.

The redox potential values of the *trans* and *cis* radical isomers are different (Table S1, ESI†). Both the complexes display two quasi-reversible redox waves due to PyCOOH/PyCOOH$^{\bullet-}$ (t-$\mathbf{2}^{rad}$, −0.85 V; c-$\mathbf{2}^{rad}$, −1.00 V) and Ru^{III}/Ru^{II} (t-$\mathbf{2}^{rad}$, +0.20 V; c-$\mathbf{2}^{rad}$, +0.42 V with respect to Fc$^+$/Fc, couple) redox couples as illustrated in Fig. S7 and S8 (ESI†). However, the PyCOOH/PyCOOH$^{\bullet-}$ couple is not stable. The redox wave due to the PyCOOH/PyCOOH$^{\bullet-}$ couple of c-$\mathbf{2}^{rad}$ diminishes faster than that of t-$\mathbf{2}^{rad}$. Both the redox waves of t-$\mathbf{2}^{rad}$ due to PyCOOH/PyCOOH$^{\bullet-}$ and Ru^{III}/Ru^{II} couples appear to be more reversible at 253 K (Fig. S8, ESI†).

The isotopic effect on the cleavage reaction was investigated using D_2O. It was observed that the reaction was facile with moist-toluene than in D_2O–toluene solvent mixtures. The cleavage reaction needs more time with D_2O. It predicts that the O–H/O–D bond cleavage leads to the C–C bond cleavage. However, the rates of transformation of c-$\mathbf{2}^{rad}$ to c-$\mathbf{3}^{ac}$ and deuterated c-$\mathbf{2_D}^{rad}$ to c-$\mathbf{3_D}^{ac}$ were compared using UV-vis/NIR spectra. It was observed that $k_H/k_D \approx 1.04$, *i.e.*, evolution of H_2 displays a secondary kinetic isotopic effect (k_H and k_D are the rates of transformation of c-$\mathbf{2}^{rad}$ to c-$\mathbf{3}^{ac}$ and c-$\mathbf{2_D}^{rad}$ to c-$\mathbf{2_D}^{ac}$). The details of these kinetic studies are given in the ESI† (page 6, Fig. S9 and S10).

$\mathbf{A}^{rad}$, t-$\mathbf{2}^{rad}$ and c-$\mathbf{2}^{rad}$ are paramagnetic while t-$\mathbf{3}^{ac}$ and c-$\mathbf{3}^{ac}\cdot\frac{1}{2}$toluene are diamagnetic. The fluid solution (CH_2Cl_2) isotropic EPR spectra at 298 K of $\mathbf{A}^{rad}$ and t-$\mathbf{2}^{rad}$ are illustrated in panels (a) and (b) of Fig. 1. The EPR spectrum of c-$\mathbf{2}^{rad}$ is displayed in Fig. S11 (ESI†). Simulations of the spectra revealed the g values and hyperfine coupling parameters. The g-values confirm the presence of organic radicals in all three complexes: $\mathbf{A}^{rad}$, g = 1.9967, $A(^{31}P)$ = 12 G; t-$\mathbf{2}^{rad}$, g = 2.002, $A(4\ ^1H)$ = 10.9 G; c-$\mathbf{2}^{rad}$, g = 2.002, $A(4\ ^1H)$ = 9.89 G. The hyperfine splitting patterns of $\mathbf{A}^{rad}$ are quite different from those of

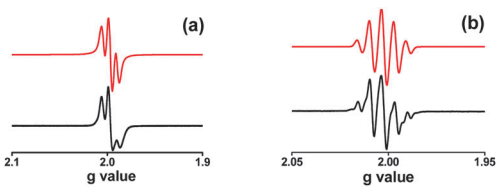

Fig. 1 (a) Hyperfine splittings of the X-band EPR spectra of (a) $\mathbf{A}^{rad}$, (b) t-$\mathbf{2}^{rad}$ (black, experimental and red, simulated spectra).

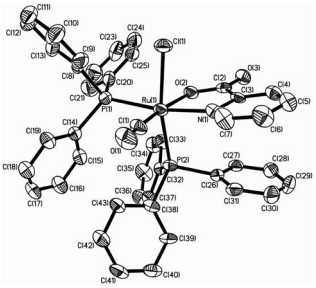

Fig. 2 ORTEP plot (30% probability level) of *c*-$\mathbf{3}^{ac}\cdot\frac{1}{2}$toluene (H atoms and solvents are excluded for clarity).

t-$\mathbf{2}^{rad}$ and *c*-$\mathbf{2}^{rad}$. The spectrum of $\mathbf{A}^{rad}$ is consistent with the presence of two equivalent PPh_3 ligands. The hyperfine couplings due to four equivalent pyridine H atoms correlate excellently with the existence of the picolinic acid anion radical in *t*-$\mathbf{2}^{rad}$ and *c*-$\mathbf{2}^{rad}$ complexes. Similar spectral features of the bipyridine anion radicals have been documented in the literature.[4]

Single crystal X-ray structure determinations have confirmed the C–C bond cleavage forming the picolinic acid from the $(PyCO)_2$ and *trans* and *cis* geometries of the *t*-$\mathbf{3}^{ac}$ and *c*-$\mathbf{3}^{ac}\cdot\frac{1}{2}$toluene complexes. However, *t*-$\mathbf{3}^{ac}$ poorly diffracts and the crystallographic data are not reported here. *c*-$\mathbf{3}^{ac}\cdot\frac{1}{2}$toluene crystallizes in the $P\bar{1}$ space group. The molecular geometry with the atom labelling scheme is illustrated in Fig. 2 (also Fig. S15, ESI†). The crystallographic data and the bond parameters of *c*-$\mathbf{3}^{ac}\cdot\frac{1}{2}$toluene are summarized in Tables S2 and S3 (ESI†) (CCDC 833917).

The spin density distributions of $\mathbf{A}^{rad}$, *t*-$\mathbf{2}^{rad}$ and *c*-$\mathbf{2}^{rad}$ were elucidated by the unrestricted DFT calculations on $[Ru(PMe_3)_2((PyCO)_2^{-\bullet})(CO)Cl]$ ($\mathbf{A}^{rad}_{Me}$), *trans*-$[Ru(PMe_3)_2(PyCOOH^{-\bullet})(CO)(Cl)]$ (*t*-$\mathbf{2}^{rad}_{Me}$) and *c*-$\mathbf{2}^{rad}$ with a doublet spin state. The gas-phase geometry of *cis*-$[Ru(PMe_3)_2(PyCOOH^{-\bullet})(CO)(Cl)]$ (*c*-$\mathbf{2}^{rad}_{Me}$) was also optimized. The optimized geometries are shown in Fig. S12 (ESI†). The calculated bond parameters of all these radical complexes are summarized in Table S4 (ESI†). *c*-$\mathbf{2}^{rad}_{Me}$ and *t*-$\mathbf{2}^{rad}_{Me}$ have comparable energies and both the isomers are isolable experimentally. Mulliken spin population analyses authenticated that the spin densities are primarily localized on the 2,2′-pyridil ligand in $\mathbf{A}^{rad}_{Me}$ and PyCOOH chelate of *t*-$\mathbf{2}^{rad}_{Me}$ and *c*-$\mathbf{2}^{rad}$. The spin density plots of $\mathbf{A}^{rad}_{Me}$, *t*-$\mathbf{2}^{rad}_{Me}$ and *c*-$\mathbf{2}^{rad}$ are shown in Fig. 3. In $\mathbf{A}^{rad}_{Me}$, spin density is mainly localized on the *trans*-CO–CO-fragment while in *t*-$\mathbf{2}^{rad}_{Me}$ and *c*-$\mathbf{2}^{rad}$ complexes it is mainly localized on the pyridine chelate forming a picolinic acid anion radical, $PyCOOH^{-\bullet}$. The spin density distribution features correlate well with the fluid solution EPR spectra of $\mathbf{A}^{rad}$ and pyridine H hyperfine couplings of *t*-$\mathbf{2}^{rad}$ and *c*-$\mathbf{2}^{rad}$ complexes at 298 K (Fig. 1).

The gas phase geometry of *cis*-$[Ru(PMe_3)_2(PyCOO^{-})(CO)(Cl)]$ (*c*-$\mathbf{3}^{ac}_{Me}$) has also been optimized with the singlet spin state for comparison. The calculated bond parameters of *c*-$\mathbf{3}^{ac}_{Me}$ are consistent with those obtained from the single crystal X-ray structure determination of *c*-$\mathbf{3}^{ac}\cdot\frac{1}{2}$toluene. It is to be noted that the experimental and calculated bond lengths of the picolinic acid anion radical are significantly different from those of the picolinate chelates (ESI,† Chart S1). The calculated C3–N1 (1.393 Å) distance of the pyridine ring of the picolinic acid anion radical is longer than that (exp., 1.339(10) Å; cal., 1.350 Å) in the picolinate chelate while the C2–C3 (1.404 Å) length in the picolinic acid anion radical is much shorter than that (exp., 1.487(12) Å; cal., 1.525 Å) in the picolinate chelate. A similar trend has been established precisely by Wieghardt *et al.* in one electron reduced iminopyridine complexes of 3d elements.[5] The C2–O2 length in the anion radical is also comparatively shorter. The C2–O3 distance (1.363 Å) is remarkably longer in the acid anion radical compared to that, 1.227(10) Å (cal., 1.231 Å), in the acid chelate. The two alternate C–C bonds in the picolinic acid anion radical (C3–C4 and C5–C6, 1.426 and 1.421 Å) are longer than the average C–C length in a pyridine ring.

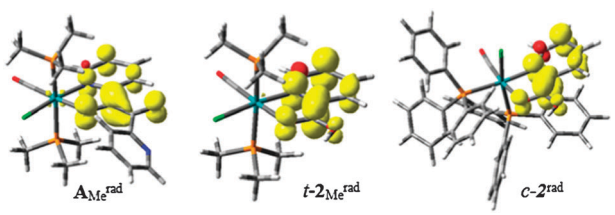

Fig. 3 Mulliken spin population analyses of $\mathbf{A}^{rad}_{Me}$, *t*-$\mathbf{2}^{rad}_{Me}$ and *c*-$\mathbf{2}^{rad}$.

The moderately strong absorption bands of *t*-$\mathbf{2}^{rad}$ and *c*-$\mathbf{2}^{rad}$ above 600 nm which are absent in picolinate complexes, *t*-$\mathbf{3}^{ac}$ and *c*-$\mathbf{3}^{ac}$, as shown in Fig. S5 (ESI†), are characteristics of a picolinic acid anion radical complex. The lower energy absorption maxima of *t*-$\mathbf{2}^{rad}$ and *c*-$\mathbf{2}^{rad}$ of LMCT origins disappear during proton induced electron transfer reaction reducing H^+ to H_2 slowly in solution as shown in Fig. S13 (ESI†). Origins of the lower energy absorptions of *t*-$\mathbf{2}^{rad}$ and *c*-$\mathbf{2}^{rad}$ have been investigated by TD DFT calculations on *t*-$\mathbf{2}^{rad}_{Me}$ and *c*-$\mathbf{2}^{rad}_{Me}$ in CH_2Cl_2 solvent using the CPCM model. The responsible photoactive orbitals are illustrated in Fig. S14 (ESI†). Calculations have predicted three lower energy absorption bands at 744.5, 709.9 and 617.6 nm due to LMCT *i.e.*, SOMO (α-HOMO) to LUMO (d_{z^2}) or LUMO + 1($d_{x^2-y^2}$) orbitals as summarized in Table S6 (ESI†). The transition features of picolinate complexes have also been elucidated by TD DFT calculation on *c*-$\mathbf{3}^{ac}_{Me}$ in dichloromethane using the CPCM model. In this case, no lower energy excitations have been predicted. The calculated lower energy excitations of *c*-$\mathbf{3}^{ac}_{Me}$ are 329.01 and 324.58 nm with oscillator strengths (*f*) of 0.015 and 0.042 respectively.

In conclusion, formation of a 2,2′-pyridil anion radical and its asymmetric cleavage by water affording unprecedented picolinic acid anion radical complexes with a transition metal ion, which produce hydrogen gas and picolinate complexes, is reported.

Financial support received from DST (SR/S1/IC/0026/2012) and CSIR (3231/NS-EMRII), New Delhi, India, is gratefully acknowledged. M. K. B. is thankful to CSIR for the fellowship (8/531(007)/2012-EMR-I). We are thankful to Prof. J. K. Bera, IIT, Kanpur, India, for providing us the facility to record hydrogen evolution.

Notes and references

1 (*a*) G. H. Spikes, E. Bill, T. Weyhermüller and K. Wieghardt, *Angew. Chem., Int. Ed.*, 2008, **47**, 2973; (*b*) G. H. Spikes, S. Sproules, E. Bill, T. Weyhermüller and K. Wieghardt, *Inorg. Chem.*, 2008, **47**, 10935.
2 M. K. Biswas, S. C. Patra, A. N. Maity, S.-C. Ke, N. D. Adhikary and P. Ghosh, *Inorg. Chem.*, 2012, **51**, 6687.
3 (*a*) W. T. Eckenhoff and R. Eisenberg, *Dalton Trans.*, 2012, **41**, 13004; (*b*) T. Lazarides, T. McCormick, P. Du, G. Luo, B. Lindley and R. Eisenberg, *J. Am. Chem. Soc.*, 2009, **131**, 9192.
4 E. Gore-Randall, M. Irwin, M. S. Denning and J. M. Goicoechea, *Inorg. Chem.*, 2009, **48**, 8304.
5 (*a*) C. C. Lu, E. Bill, T. Weyhermüller, E. Bothe and K. Wieghardt, *J. Am. Chem. Soc.*, 2008, **130**, 3181; (*b*) A. C. Bowman, C. Milsmann, C. C. H. Atienza, E. Lobkovsky, K. Wieghardt and P. J. Chirik, *J. Am. Chem. Soc.*, 2010, **132**, 1676.